RAPID COMMUNICATION

Manipulation of extraordinary acoustic transmission by a tunable bull's eye structure*

Wang Ji-Wei(王继伟)[a], Cheng Ying(程 营)[a)b)†], and Liu Xiao-Jun(刘晓峻)[a)b)‡]

[a] Key Laboratory of Modern Acoustics, Nanjing University, Nanjing 210093, China
[b] State Key Laboratory of Acoustics, Institute of Acoustics, Chinese Academy of Sciences, Beijing 100190, China

(Received 1 November 2013; revised manuscript received 2 December 2013; published online 1 April 2014)

Extraordinary acoustic transmission (EAT) has been investigated in a tunable bull's eye structure. We demonstrate that the transmission coefficient of acoustic waves can be modulated by a grating structure. When the grating is located at a distance of 0.5 mm from the base plate, the acoustic transmission shows an 8.77-fold enhancement compared to that by using a traditional bull's eye structure. When the distance increases to 1.5 mm, the transmission approaches zero, indicating a total reflection. Thus, we can make an efficient modulation of acoustic transmission from 0 to 877%. The EAT effects have been ascribed to the coupling of structure-induced resonance with the diffractive wave and the waveguide modes, as well as the Fabry–Perot resonances. As a potential application, the modulation of far-field collimation is illustrated in the proposed bull's eye structure.

Keywords: extraordinary acoustic transmission, acoustic grating, transmission modulation, sound collimation

PACS: 43.20.Fn, 43.20.El, 43.20.Ks, 43.35.–c **DOI:** 10.1088/1674-1056/23/5/054301

1. Introduction

Metamaterials have gained extensive attention due to their ability to exhibit many unnatural and fascinating phenomena that are impossible to obtain in natural materials.[1] Optical metamaterials have shown many applications, such as extraordinary optical transmission (EOT),[2–11] optical superlensing,[12,13] and invisibility optical cloaking.[14] On the other hand, acoustic metamaterials have been proposed to have many potential applications, such as extraordinary acoustic transmission (EAT),[15–24] collimation and focusing,[25–27] acoustic cloaking,[28,29] sonar sensing,[30] and acoustic filter.[31–33]

Acoustic grating has been widely used to tune many aspects of acoustic transmission, such as the realization of unidirectional acoustic transmission,[34–36] extremely flat transmission under oblique incidence,[37] and the EAT.[15–17] The EAT phenomenon has been intensely investigated in many structures, such as single subwavelength aperture surrounded by finite periodic grooves and a one-dimensional grating.[15–22] Zhang[15] obtained the EAT through acoustic gratings with very narrow slits by multiple-scattering numerical simulations. The resonant transmission has been ascribed to the excitation of transverse and coupled resonant acoustic modes along the direction of grating period. Lu *et al.*[16] experimentally demonstrated the EAT phenomena through 1D acoustic gratings with subwavelength apertures. The physical origin of the EAT is attributed to the strong coupling between the diffractive surface wave and waveguide modes. Christensen *et al.*[17] presented a complete study of the acoustic transmission properties of subwavelength apertures. When the apertures are placed in a periodic fashion, a new type of transmission resonance appears in the spectrum. They have demonstrated that this resonance stems from the excitation of an acoustic guided wave that hybridizes strongly with the FP resonances associated with waveguide modes in single apertures. However, the EAT phenomenon only occurs at particular frequencies and it cannot be modulated in the traditional grating structure.

In this paper, we have proposed a tunable grating with an asymmetric bull's eye structure that can modify the acoustic transmission coefficient. An efficient modulation of acoustic transmission from 0 to 877% has been demonstrated. We have further found two kinds of EAT effects. One is attributed to the coupling of structure-induced resonance with the diffractive wave and the waveguide mode, and the other is due to the FP resonances between the grating and the base plate. As a potential application, the modulation of far-field collimation is illustrated in the proposed bull's eye structure.

2. Simulation results and discussion

Figure 1(a) illustrates a cross-section view of the proposed tunable bull's eye structure, which consists of a periodic rectangular grating and a base plate with a single cen-

*Project supported by the National Basic Research Program of China (Grant No. 2012CB921504), the National Natural Science Foundation of China (Grant Nos. 11104139, 11274171, 11274099, and 11204145), SRFDP (Grant Nos. 20110091120040, 20120091110001, and 20130091130004), and the Natural Science Foundation of Jiangsu Province, China (Grant No. BK2011542).

†Corresponding author. E-mail: chengying@nju.edu.cn
‡Corresponding author. E-mail: liuxiaojun@nju.edu.cn

© 2014 Chinese Physical Society and IOP Publishing Ltd

tral aperture. The thickness of the base plate and width of the aperture are $w = 1.5$ mm and $a = 0.5$ mm, respectively. The thickness of the grating is $h = 0.5$ mm, and the period is $d = 3.0$ mm. The distance between the grating and base plate H can be tuned. When $H = 0$ mm, this structure degenerates into a traditional asymmetric bull's eye structure.[17] In this study, the fluid medium is selected to be water with a density of $\rho_w = 998$ kg/m^3 and the sound velocity is set as $c_w = 1483$ m/s. The metal plate is assumed to be rigid and the acoustic impedance significantly mismatches with that of water. The structure consists of 32 periods and is excited by a monochromic source.

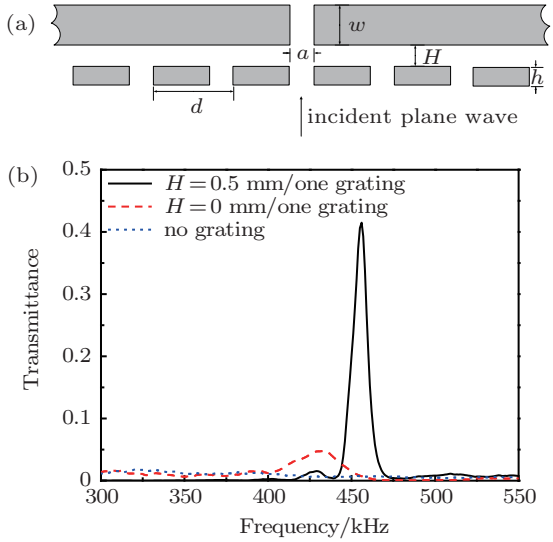


Fig. 1. (a) Tunable bull's eye structure consisting of a periodic grating and a base plate with a central aperture. The thickness of the base plate and the width of the aperture are $w = 1.5$ mm and $a = 0.5$ mm, respectively. The thickness of the grating is $h = 0.5$ mm, and the period is $d = 3.0$ mm. The grating consists of 32 periods. The distance H between the grating and the base plate is a configurable parameter. (b) Transmittance with different H values: 0.5 mm (solid curve), 0 mm (dashed curve), and no grating (dotted curve).

First, we investigate the influence of H on the acoustic transmittance. We assume that an acoustic plane wave impinges normally onto the structure, and the incident frequency sweeps from 300 kHz to 550 kHz. By using full-wave simulations, the variation of the acoustic transmittance for the asymmetric bull's eye structures with different H values is shown in Fig. 1(b). Transmission peaks are observed in both regular bull's eye structure with $H = 0$ mm (dashed curve) and modulated version with $H = 0.5$ mm (solid curve), while no obvious peak exists for a pure plate without grating (dotted curve). For the case of $H = 0.5$ mm, the transmission peak is significantly higher than that for the other two cases. The peak intensity ($T = 0.4158$) for the case of $H = 0.5$ mm has an 8.77-fold enhancement compared to that ($T = 0.0474$) for the case of $H = 0$ mm, and a 62.06-fold enhancement compared to that ($T = 0.0067$) without grating structure. The T value (~ 0.4158) for the case of $H = 0.5$ mm is significantly improved compared to that ($T = 0.0474$) for the regular bull's eye structure ($H = 0$ mm), suggesting an enhanced EAT effect. It is noted that the resonant frequency is slightly shifted from 432 kHz for the case of $H = 0$ mm to 456 kHz for the case of $H = 0.5$ mm. This can be ascribed to the variation of the resonance of structure-factor-induced surface modes and coherent diffraction in the EAT.[17,18]

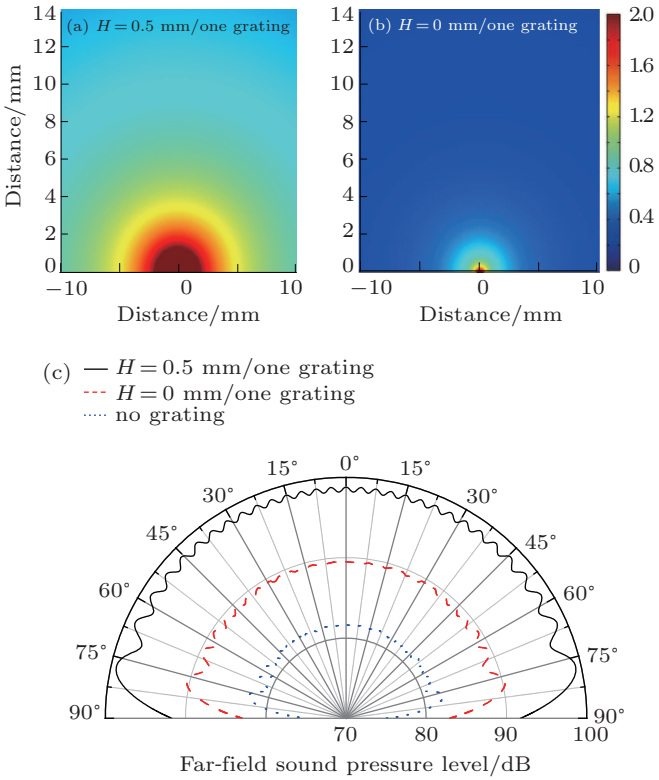


Fig. 2. Far-field spatial distribution of the pressure field at the output side of the structure: (a) $H = 0.5$ mm at 456 kHz. (b) $H = 0$ mm at 432 kHz. (c) The angle distribution of the energy at the output side for $H = 0.5$ mm (solid curve), $H = 0$ mm (dashed curve), and no grating (dotted curve).

In order to confirm the manipulation EAT effects as shown in Fig. 1(b), we further calculate the far-field spatial distributions of the pressure fields at the output sides of the structures. In Fig. 2, it is found that the acoustic transmission for $H = 0.5$ mm (Fig. 2(a)) is much stronger than that for $H = 0$ mm (Fig. 2(b)). We further investigate the angle distribution of the acoustic transmission, the extracted directivity diagrams at the output sides are shown in Fig. 2(c). The solid, dashed, and dotted curves represent the cases of $H = 0.5$ mm, $H = 0$ mm, and plate without grating, respectively. All the results are plotted in log scale. For the case of plate without grating, the low transmission is about 81.6 dB and the near-ideal isotropic sound radiation emits uniformly in directions from 0° to 75° (dotted curve in Fig. 2(c)). When the grating structure is attached to the input surface of the plate, the transmitted acoustic wave is dramatically enhanced by 7.9 dB in almost all directions (dashed curve in Fig. 2(c)). Furthermore, the transmission increases to about 98.8 dB when the grating is moved to a distance of $H = 0.5$ mm from the base plate (solid curve in

Fig. 2(c)). The acoustic radiation is almost equally improved by 9.3 dB in all directions compared to that of the case for $H = 0$. When H becomes zero, the sound pressure level L_{P_0} along the axis direction is 89.5 dB, while the sound pressure level $L_{P_{0.5}}$ is 98.8 dB when $H = 0.5$ mm. Thus, an 851% enhancement of the sound transmittance is achieved, according to the ratio of $I_{P_{0.5}}/I_{P_0} = 10^{(L_{P_{0.5}} - L_{P_0})/10}$=8.51, which is almost in agreement with that (877%) calculated in Fig. 1(b).

In order to investigate the effective manipulation character of the proposed approach, we further investigate the evolution of transmitted sound with the variation of H from 0 to 3 mm. In Fig. 3(a), we find two EAT lines: a horizontal line and an inclined line. For the horizontal line, it is found that the resonant frequency shifts from 432 kHz to 461 kHz when the H value increases from 0 to 3 mm (square curve in Fig. 3(b)). This behavior is analogous to the locally-resonant frequency in metamaterials composed of coupled microstructures, and should be attributed to the coupling of structure-induced resonance with the diffractive wave and the waveguide mode. Moreover, the resonant frequency for the inclined line greatly decreases from 450 kHz for $H \sim 1.6$ mm to 300 kHz for $H \sim 2.4$ mm (circle curve in Fig. 3(b)). The corresponding wavelength increases from 3.30 mm to 4.94 mm, which is about twice the distance H, indicating the first-order FP resonance. Similarly, when H increases from 2.7 mm to 3.0 mm, the resonant frequency decreases from 550 kHz to 500 kHz (triangle curve in Fig. 3(b)), and the corresponding wavelength is roughly equivalent to the distance H, suggesting the second-order FP resonance. It is further found that the transmittance maintains a high value in the range of $H = 0.3$–1.2 mm, and then decreases to a low value at other H values, as shown in Fig. 3(a). Figure 3(c) shows the dependence of the transmittance on the H values. For the horizontal line, the transmittance gradually increases from 0.05 at $H = 0$ mm to 0.4158 at $H = 0.5$ mm, and then decreases to 0 at $H = 1.5$ mm, as shown by the square curve in Fig. 3(c). With further increase of the H value from 1.5 mm to 3.0 mm, the transmittance suddenly increases to ~ 0.07. It is surprising that the transmission ($T \sim 0$) is almost perfectly inhibited when $H = 1.5$ mm, which is even lower than that ($T = 0.0067$) for the plate with a single aperture. In the range of H values from 0.3 mm to 1.2 mm, we find intensive resonance in the aperture of the base plate. Meanwhile, the resonance in the aperture of the base plate becomes weak at other H values, especially at $H = 1.5$ mm. Thus, the resonance in the aperture of the base plate plays an important role in acoustic transmission. Therefore, we can not only enhance but also isolate the acoustic transmission by changing the distance between the grating and the base plate. In addition, for the inclined line, the transmittance due to the first-order FP resonance decreases from 0.067 for $H = 1.6$ mm to 0.029 for $H = 1.8$ mm, and then increases to 0.11 for $H = 2.4$ mm, as shown by the circle curve in Fig. 3(c). The transmittance due to the second-order FP resonance decreases from 0.067 for $H = 2.7$ mm to 0.015 for $H = 3.0$ mm, as shown by the triangle curve in Fig. 3(c). We further compare the contribution of FP resonance and the coupling modes between the diffractive wave and the waveguide modes on the EAT. As shown in Fig. 3(c), the coupling modes between the diffractive wave and the waveguide mode play a main role on the EAT in the range of H values from 0 mm to 1.5 mm. In the range of H values from 1.5 mm to 3.0 mm, both the coupling modes between the diffractive wave and the waveguide mode and the FP resonance contribute to the EAT.

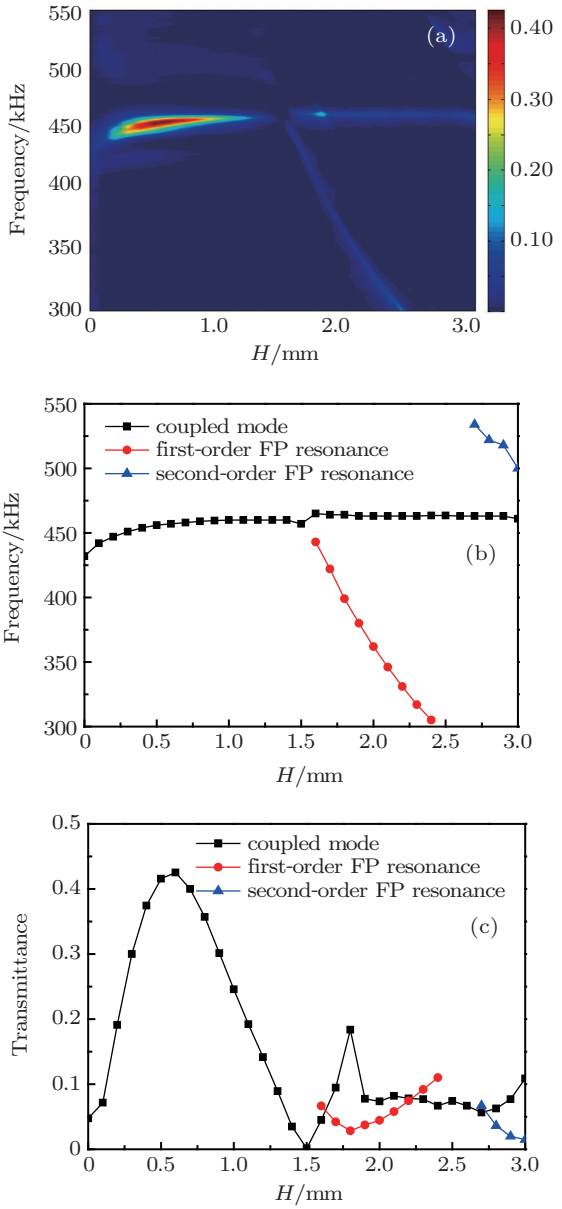


Fig. 3. (a) Evolution of the transmittance with H. (b) Dependence of the resonant frequency on H. (c) Dependence of the intensity for the transmission peak on H.

We further investigate the surface acoustic waves induced by the tunable grating structure and the eigenmodes through the pressure field distribution in the unit cells of the composite structure. Figure 4 shows the near-field pressure amplitude

distributions for the cases of the regular bull's eye ($H = 0$ mm at 432 kHz), $H = 0.5$ mm at 456 kHz, and $H = 1.5$ mm at 456 kHz. Here, the arrows represent the vibration velocity, and the scale factor of the arrows in Fig. 4(c) is magnified by five times. We note that a local resonance exists in all three cases. Although the pressure amplitude inside the grooves is very high (e.g., ~14 times of the amplitude of the incident wave), the intensity of the surface wave is weak and the transmitted energy through the central aperture is low for the case of $H = 0$ mm (see Fig. 4(a)). For the case of $H = 0.5$ mm (see Fig. 4(b)), the intensive resonances are investigated not only between each grating, but also between the gratings and the base plate. The diffractive wave is also found to be excited by the grating and the waveguide modes coupling with each other, which leads to the circular vibration around the rectangular gratings. The separation of the plate and the grating opens an additional effective propagation path for surface acoustic waves, and then more energy can be gathered, thereby enhancing the acoustic transmission through the central aperture. In addition, the induced resonances can also isolate the transmission when they are not coupled with each other, as shown in Fig. 4(c). The velocity around the grating becomes very small compared to that for the case of $H = 0$ mm or 0.5 mm. We have further found that the stronger the resonances couple with each other are, the more intensive the resonance in the aperture of the base plate will be, and hence the higher acoustic transmission.

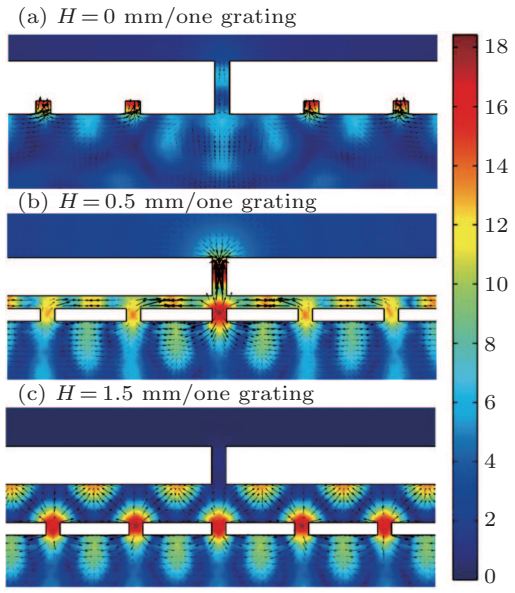


Fig. 4. Near-field spatial distribution of the pressure field at the input side of the structure: (a) $H = 0$ mm at 432 KHz; (b) $H = 0.5$ mm at 456 KHz; (c) $H = 1.5$ mm at 456 KHz. The direction (size) of the arrows indicates the direction (magnitude) of vibration velocity. Note that the scale factor of the arrows in (c) is magnified by five times.

Finally, a possible application of the manipulation approach in sound collimation is discussed. In Fig. 5, another grating is placed in front of the output side of the base plate in the asymmetric bull's eye structure. Here, the material and geometric parameters of the output grating are the same as that of the input one, and the distance between the base plate and the output grating is H. According to Christensen's theory, the regular bull's eye structure has the ability to achieve extraordinary acoustic transmission and strong collimation.[21] Thus, the grating on the input surface allows for the coupling of surface modes, while the grating on the output surface determines the beam shape and angle.[26] In our proposed structure, the far-field acoustic pressure field for the case of $H = 0$ mm at 430 kHz is shown in Fig. 6(a). It is found that the acoustic surface waves are excited, which is accompanied by the acoustic resonant transmission in the structure. Then, the acoustic surface waves are scattered by the grooves, which further couple with the transmitted wave from the slit, forming the collimated beam in the far-field region. In the case of $H = 0.5$ mm at 456 kHz, a significant enhancement of the collimated beam is observed in the far field, as shown in Fig. 6(b). The origin of the enhanced collimation phenomenon is ascribed to the detached gratings, which induces the scattered waves stronger and hence the larger coupling with the diffracted waves. As a reference, the far-field acoustic pressure field for the case of grating only on the input side ($H = 0.5$ mm) at 456 kHz is shown in Fig. 6(c), in which the collimation phenomenon disappears. We also exhibit the corresponding directivity diagram at the output side of the structure in Fig. 6(d). The maximum pressure amplitudes are determined to be 114.72 dB and 102.14 dB along the direction of 0° for the two gratings of $H = 0.5$ mm and $H = 0$ mm, respectively. The far-field energy-flow density along the direction of 0° for $H = 0.5$ mm is improved by 18.11 times compared to the regular bull's eye ($H = 0$ mm). In addition, the sound beam is found to have a narrow angular region with a full width at half maximum (FWHM) of 3.55° for the case of $H = 0.5$ mm, which is only one third of that (FWHM=10.25°) for the case of $H = 0$ mm, as shown in Fig. 6(d). In contrast, for the case of one grating at the input side ($H = 0.5$ mm), the sound energy exhibits uniform distribution in directions from 0° to 75° with a pressure amplitude of 98.8 dB, as shown by the dotted cave in Fig. 6(d). Thus, a significant improvement for superdirectivity has been observed in the proposed bull's eye structure.

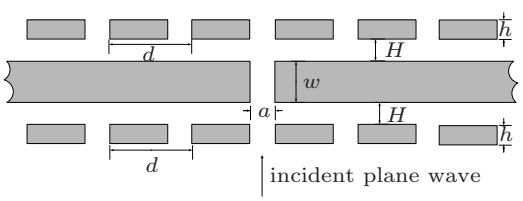


Fig. 5. Tunable symmetric bull's eye structure with two acoustic gratings at the input and output sides.

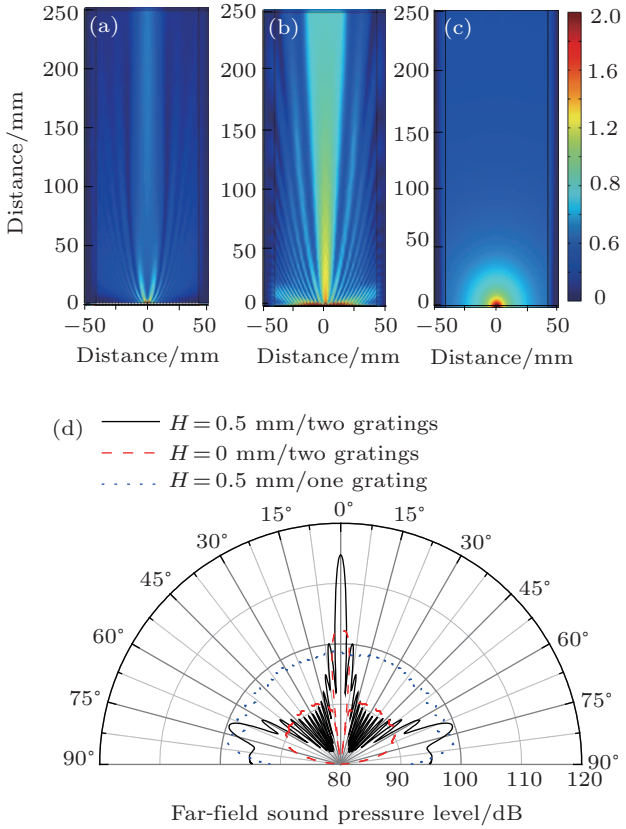


Fig. 6. Far-field spatial distribution of the pressure field at the output side of the structure at the resonance frequency: (a) $H = 0$ mm with two acoustic gratings; (b) $H = 0.5$ mm with two acoustic gratings; and (c) $H = 0.5$ mm with one grating. (d) Angle distribution of the energy in the output side for $H = 0.5$ mm with two gratings (solid curve), $H = 0$ mm with two gratings (dashed curve), and $H = 0.5$ mm with one grating (dotted curve).

3. Conclusion

We have reported a manipulation of the extraordinary acoustic transmission (EAT) by a tunable bull's eye structure. The efficient modulation of EAT can be changed from 0 to 877%. The EAT effects have been ascribed to the coupling of structure-induced resonance with the diffractive wave and the waveguide mode, as well as the Fabry–Perot resonances. We also demonstrate the enhanced collimation effect in the bull's eye structure. This approach has shown potential applications in ultrasonic focusing and detection.

References

[1] Liu Z Y, Zhang X X, Mao Y W, Zhu Y Y, Yang Z Y, Chan C T and Sheng P 2000 *Science* **289** 1734

[2] Ebbesen T W, Lezec H J, Ghaemi H F, Thio T and Wolff P A 1998 *Nature* **391** 667

[3] Martín-Moreno L, García-Vidal F J, Lezec H J, Pellerin K M, Thio T, Pendry J B and Ebbesen T W 2001 *Phys. Rev. Lett.* **86** 1114

[4] Barnes W L, Dereux A and Ebbesen T W 2003 *Nature* **424** 824

[5] Liu H and Lalanne P 2008 *Nature* **452** 728

[6] Bao Y J, Peng R W, Shu D J, Wang M, Li X, Shao J, Lu W and Ming N B 2008 *Phys. Rev. Lett.* **101** 087401

[7] Huang X R, Peng R W and Fan R H 2010 *Phys. Rev. Lett.* **105** 243901

[8] Li J Y, Hua Y L, Fu J X and Li Z Y 2010 *J. Appl. Phys.* **107** 073101

[9] Rodrigo Sergio G, García-Vidal F J and Martín-Moreno L 2008 *Phys. Rev. B* **77** 075401

[10] Wu C N, Li H J, Peng X, Cao G T and Liu Z M 2013 *Chin. Phys. B* **22** 057301

[11] Wei F F, Wang H Y and Zhou Y S 2013 *Chin. Phys. B* **22** 024201

[12] Zhang X and Liu Z W 2008 *Nat. Mater.* **7** 435

[13] Pendry J B 2000 *Phys. Rev. Lett.* **85** 3966

[14] Pendry J B, Schrurig D and Smith D R 2006 *Science* **312** 1780

[15] Zhang X D 2005 *Phys. Rev. B* **71** 241102

[16] Lu M H, Liu X K, Feng L, Li J, Huang C P, Chen Y F, Zhu Y Y, Zhu S N and Ming N B 2007 *Phys. Rev. Lett.* **99** 174301

[17] Christensen J, Martin-Moreno L and Garcia-Vidal F J 2008 *Phys. Rev. Lett.* **101** 014301

[18] Zhou Y, Lu M H, Feng L, Ni X, Chen Y F, Zhu Y Y, Zhu S N and Ming N B 2010 *Phys. Rev. Lett.* **104** 164301

[19] Christensen J, Martín-Moreno L and García-Vidal F J 2010 *Phys. Rev. B* **81** 174104

[20] Mei J, Hou B, Ke M, Peng S, Jia H, Liu Z, Shi J, Wen W and Sheng P 2008 *Appl. Phys. Lett.* **92** 124106

[21] Christensen J, Fernandez-Dominguez A I, de Leon-Perez F, Martin-Moreno L and Garcia-Vidal F J 2007 *Nat. Phys.* **3** 851

[22] Hou B, Mei J, Ke M, Wen W, Liu Z Y, Shi J and Sheng P 2007 *Phys. Rev. B* **76** 054303

[23] He Z J, Jia H, Qiu C Y, Peng S S, Mei X F, Cai F Y, Peng P, Ke M Z and Liu Z Y 2010 *Phys. Rev. Lett.* **105** 074301

[24] Qi D X, Fan R H, Peng R W, Huang X R, Lu M H, Ni X, Hu Q and Wang M 2012 *Appl. Phys. Lett.* **101** 061912

[25] Zhang S, Yin L and Fang N 2009 *Phys. Rev. Lett.* **102** 194301

[26] Cheng Y, Xu J Y and Liu X J 2010 *Appl. Phys. Lett.* **96** 071910

[27] Wei Q, Cheng Y and Liu X J 2011 *Acta Phys. Sin.* **60** 124301 (in Chinese)

[28] Chen H Y and Chan C T 2007 *Appl. Phys. Lett.* **91** 183518

[29] Shen H J, Wen J H, Yu D L, Cai L and Wen X S 2012 *Acta Phys. Sin.* **61** 134303 (in Chinese)

[30] Estrada H, Candelas P, Uris A, Belmar F, Garcia de Abajo F J and Meseguer F 2008 *Phys. Rev. Lett.* **101** 084302

[31] Ding H X, Shen Z H, Ni X W and Zhu X F 2012 *Appl. Phys. Lett.* **100** 083501

[32] Wang J S, Xu X D, Liu X J and Xu G C 2009 *Appl. Phys. Lett.* **94** 181908

[33] Gao D B, Zeng X W, Zhou Z M and Tian Z F 2013 *Acta Phys. Sin.* **62** 094304 (in Chinese)

[34] He Z J, Peng S S, Ye Y T, Dai Z W, Qiu C Y, Ke M Z and Liu Z Y 2011 *Appl. Phys. Lett.* **98** 083505

[35] Jia H, Ke M Z, Li C H, Qiu C Y and Liu Z Y 2013 *Appl. Phys. Lett.* **102** 153508

[36] Xu S J, Qiu C Y and Liu Z Y 2012 *J. Appl. Phys.* **111** 094505

[37] Qi D X, Fan R H, Peng R W, Huang X R, Lu M H, Ni X, Hu Q and Wang M 2012 *Appl. Phys. Lett.* **101** 061912